Molecular Microbiology (2008) 69(2), 548–558 ■
doi:10.1111/j.1365-2958.2008.06307.x
First published online 9 June 2008

# Repression of motility during fimbrial expression: identification of 14 *mrpJ* gene paralogues in *Proteus mirabilis*

**Melanie M. Pearson and Harry L. T. Mobley***
*Department of Microbiology and Immunology, University of Michigan Medical School, Ann Arbor, MI 48109–0620, USA.*

## Summary

***Proteus mirabilis*** **alternates between motile and adherent forms. MrpJ, a transcriptional regulator previously reported to repress motility, is encoded at the 3′ end of the *mrp* fimbrial operon in *P. mirabilis*. Sequencing of the *P. mirabilis* genome revealed 14 additional paralogues of *mrpJ*, 10 of which are associated with fimbrial operons. Twelve of these genes, when overexpressed, repressed motility; several distinct patterns of swarming motility were noted. Expression of 10 of the 14 *mrpJ* paralogues repressed flagellin (FlaA) synthesis. Alignment of the predicted amino acid sequences of MrpJ and its 14 paralogues revealed a conserved consensus motif (SQQQFSRYE) within the helix-turn-helix domain. Site-directed mutagenesis of these residues coupled with linker insertion mutagenesis of MrpJ confirmed the importance of this domain for repression of motility. Gel shift assays demonstrated that MrpJ and another paralogue UcaJ bind directly to the promoter region of the flagellar master regulator *flhDC*. Thus, *P. mirabilis* appears to use a related mechanism to inhibit motility during the production of at least 10 of its predicted fimbriae.**

## Introduction

Motility and attachment represent opposing aspects of the life cycles of many bacterial species, yet both contribute to bacterial fitness and virulence in the host. As might be expected, both systems are subject to complex regulation. Bacterial motility is mediated by the flagellum, and attachment by fimbriae (Finlay and Falkow, 1997). However, only a few regulatory networks have been found that simultaneously increase fimbrial expression while decreasing flagellum-mediated motility, or vice versa. These include the *bvgAS* system of *Bordetella* species (Akerley *et al.*, 1995), the messenger cyclic di-GMP (Simm *et al.*, 2004), *fimZ* expression in *Salmonella enterica* serovar Typhimurium (Clegg and Hughes, 2002) and motility feedback into the ToxR regulatory system in *Vibrio cholerae* (Gardel and Mekalanos, 1996). Constitutive expression of type 1 fimbriae in uropathogenic *Escherichia coli* has also been shown to decrease swimming motility (Bryan *et al.*, 2006; Lane *et al.*, 2007). Another strategy for decreasing motility while fimbriae are expressed is mediated by *mrpJ*, a gene located at the end of the mannose-resistant *Proteus*-like (MR/P) fimbrial operon which when overexpressed, decreases flagellum-mediated motility in *Proteus mirabilis* (Li *et al.*, 2001).

*Proteus mirabilis*, a member of the *Enterobacteriaceae* and an opportunistic pathogen of the urinary tract, frequently infects patients with indwelling urinary catheters (reviewed in Coker *et al.*, 2000). This organism has long been studied for its ability to swarm across solid surfaces (reviewed in Rather, 2005), during which short, vegetative swimmer cells convert to very long (up to 100 μm), hyperflagellated swarmer cells. These swarmer cells also exhibit reduced expression of fimbriae (Mobley *et al.*, 1996; Jansen *et al.*, 2003), suggesting possible co-ordinate expression between flagella and fimbriae. Prior to the sequencing of the *P. mirabilis* genome, expression of five different fimbriae had been documented in *P. mirabilis*: MR/P fimbriae (Adegbola *et al.*, 1983; Bahrani *et al.*, 1994), uroepithelial cell adhesin (UCA, also known as non-agglutinating fimbriae or NAF) (Wray *et al.*, 1986; Cook *et al.*, 1995), *P. mirabilis* fimbriae (PMF) (Adegbola *et al.*, 1983; Massad *et al.*, 1994a), ambient temperature fimbriae (ATF) (Massad *et al.*, 1994b) and *P. mirabilis* P-like pili (PMP) (Bijlsma *et al.*, 1995). The MR/P fimbria is encoded by an operon containing nine genes (Bahrani *et al.*, 1994). The last gene in the *mrp* operon is *mrpJ*, which encodes a helix-turn-helix (HTH) xenobiotic response element (XRE) family transcriptional regulator (Li *et al.*, 2001).

Subsequent to our initial report of MrpJ control of both swimming and swarming motility and its functional

Accepted 14 May, 2008. *For correspondence. E-mail hmobley@umich.edu; Tel. (+1) 734 764 1466; Fax (+1) 734 763 7163.

**Table 1.** *mrpJ* paralogues in *P. mirabilis* HI4320.

| Name | Locus | Fimbrial operon |
|---|---|---|
| *mrpJ′* | PMI0261 | MR/P′ |
| *mrpJ* | PMI0271 | MR/P |
| *fim3J* | PMI0296 | Fimbria 3 |
| *ucaJ* | PMI0532 | UCA |
| *fim5J* | PMI1060 | Fimbria 5 |
| *fim8J* | PMI1470 | Fimbria 8 |
| *fim10J1* | PMI2209 | Fimbria 10 |
| *fim10J2* | PMI2207 | Fimbria 10 |
| *pmpJ* | PMI2224 | PMP |
| *atfJ* | PMI2733 | ATF |
| *fim14J* | PMI3003 | Fimbria 14 |
| PMI0182 | PMI0182 | Orphan |
| PMI0982 | PMI0982 | Orphan |
| PMI1817 | PMI1817 | Orphan |
| PMI3508 | PMI3508 | Orphan |

homologue *papX* in *E. coli* (Li *et al.*, 2001), *mrpJ* homologues have been found associated with fimbrial operons in *Xenorhabdus nematophila* (He *et al.*, 2004) and *Photorhabdus temperata* (Meslet-Cladiere *et al.*, 2004), although the phenotype of these *mrpJ* homologues on motility has not yet been established. However, the recent completion of the *P. mirabilis* genome (Pearson *et al.*, 2008) predicted that this organism has 14 additional *mrpJ* paralogues, most of which (10 of 14) are also associated with fimbrial operons. This report details the role of all 15 *P. mirabilis mrpJ*-like genes in both swimming and swarming motility, and presents data on the mechanism of MrpJ action.

## Results

### Proteus mirabilis *HI4320 has 14 additional* mrpJ *homologues*

The recent annotation of the *P. mirabilis* genome (Pearson *et al.*, 2008) revealed 17 potential chaperone-usher fimbrial operons. Surprisingly, 10 of these 17 operons contain an *mrpJ* paralogue either at the beginning (five paralogues) or the end (five paralogues) of the operon (Table 1). One operon, *fimbria10*, has two *mrpJ* paralogues. A further scan of the genome located four additional *mrpJ* paralogues that do not appear to be associated with fimbrial genes (denoted as orphans in Table 1).

### *The majority of the* mrpJ *paralogues repress motility when overexpressed*

Each of the 14 *mrpJ* paralogues was cloned into the IPTG-inducible plasmid vector pLX3607. *P. mirabilis* HI4320 was electroporated with the *mrpJ* paralogue clones, and flagellar motility was examined (Fig. 1). Strain HI4320 overexpressing *mrpJ* or its paralogues was stabbed into soft agar to measure swimming motility (Fig. 1A). The IPTG-inducible promoter in pLX3607 drives a low level of expression in the absence of IPTG; this level of *mrpJ* paralogue expression was sufficient to significantly reduce swimming motility in 11 of the 14 *mrpJ* paralogue overexpression strains ($P < 0.05$). When expression was induced with 0.3 mM IPTG, 12 of the 14 *mrpJ* paralogue overexpression strains were less motile compared with the induced vector control ($P < 0.05$) (Fig. 1A). Although statistically significant, the slight reduction of motility for the PMI0182 and PMI0982 overexpression strains in the presence of IPTG when compared with the induced vector control is likely not biologically significant.

To measure the effect of *mrpJ* paralogue overexpression strains on swarming across surfaces, cultures of these strains were spotted onto the centre of swarm agar plates. Eight of the 14 strains displayed reduced swarming motility compared with the vector control without IPTG induction ($P < 0.05$) (Fig. 1B). When overexpression was induced with IPTG, 10 of the 14 strains (i.e. two additional paralogues) were significantly less motile than the vector ($P < 0.05$).

### *Overexpression of most* mrpJ *paralogues reduces expression of flagellin in broth culture*

Overexpression of *mrpJ* causes a reduction in the level of the major flagellin FlaA in *P. mirabilis* (Li *et al.*, 2001). To test whether this was the case for the other 14 *mrpJ* paralogues in *P. mirabilis* HI4320, whole-cell lysates of stationary phase HI4320 expressing each of these paralogues in plasmid pLX3607 were analysed by Western blot for FlaA expression (Fig. 2). Overexpression of *mrpJ* paralogues resulted in a wide range of FlaA expression, with most having visibly less FlaA expression. The *fim10J1*, *pmpJ*, PMI0182 and PMI0982 overexpression constructs, however, had FlaA expression levels similar to the vector control. The same alterations in FlaA expression were observed when Western blot analysis of the strains shown in Fig. 3 was conducted on mid-logarithmic phase cultures (data not shown).

### *Overexpression of some* mrpJ *paralogues inhibits normal swarm cell differentiation*

In addition to reduced overall motility, at least four different swarm patterns were observed in HI4320 overexpressing *mrpJ* or *mrpJ* paralogues (Fig. 3). Not only did some strains fail to exhibit the classic 'bulls-eye' swarming pattern of *P. mirabilis*, but radial growth (*mrpJ*), thin films (*ucaJ*) or disorganized swarming (*pmpJ*) was observed. In contrast, overexpression of PMI0982 resulted in swarm rings of larger diameter as compared with the vector control (Fig. 3A).

 

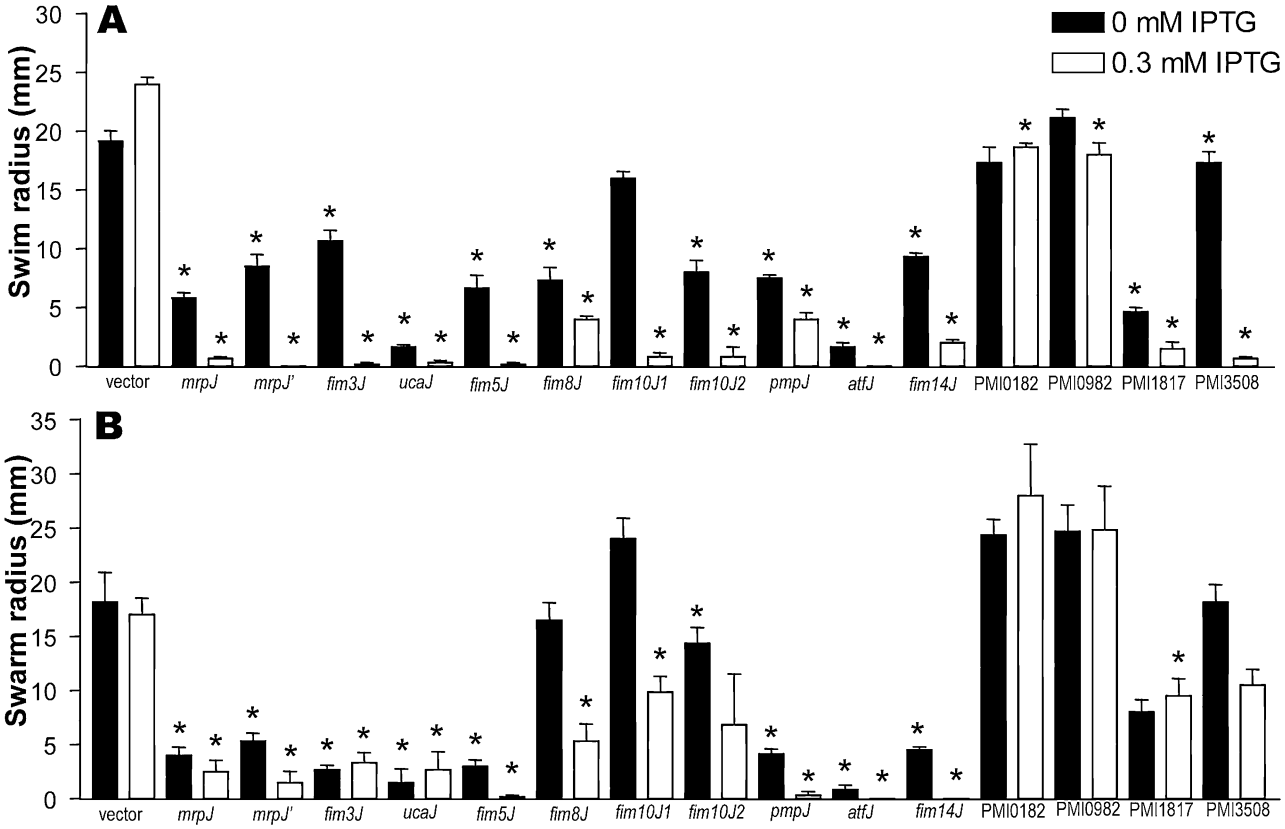


**Fig. 1.** Swimming and swarming motility of *P. mirabilis* when *mrpJ* or its paralogues are overexpressed.
A. Swimming radius of strains stabbed in soft agar.
B. Swarming radius of strains spotted on swarm agar. In both A and B, black bars represent the swim or swarm radius of uninduced strains, while white bars represent strains that were induced with IPTG. Error bars represent the standard error of the mean. Asterisks indicate $P < 0.05$ when compared with the vector control.

To investigate whether these strains were not swarming as a result of an inability to differentiate into swarmer cells, Gram stains were prepared from the edge of swarm fronts and imaged by light microscopy (Fig. 3B). *P. mirabilis* from the edge of the vector control or the PMI0982 swarm had differentiated into swarmer cells of various lengths. Strains overexpressing *mrpJ* and *pmpJ* were found to have mixed populations of normal-appearing swarm cells and much shorter cells. Surprisingly, the strain overexpressing *ucaJ* was a uniform population of very long swarmer cells (Fig. 3B), although this strain exhibits almost no swarming motility (Fig. 3A).

### *Overexpression of* mrpJ *or* mrpJ *paralogues results in altered fimbrial and flagellar structures*

To examine the effect of overexpression of *mrpJ* or *mrpJ* paralogues on individual bacteria in a population, overnight cultures of the strains assessed in Fig. 3 were prepared for transmission electron microscopy (TEM) and representative fields were selected. As expected, overexpression of *mrpJ* or *ucaJ* led to a marked decrease in the number of bacteria that possessed flagella (Fig. 4B and C). However, although the strain that overexpressed *pmpJ* had apparently normal levels of FlaA flagellin

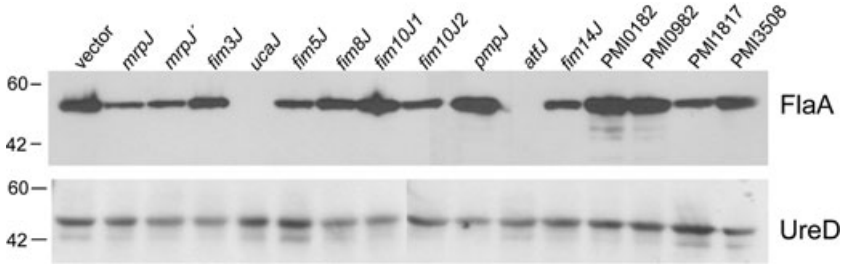


**Fig. 2.** Western blot of flagellin expression in *P. mirabilis mrpJ* or *mrpJ* paralogue overexpression strains. Whole-cell lysates of uninduced strains were denatured, electrophoresed on 10% SDS-PAGE and blotted with anti-FlaA antibody, which recognizes the major subunit of the flagellum. Lysates were also blotted with anti-UreD antibody as a loading control (lower panel). Molecular weight markers are indicated on the left side in kDa.

 

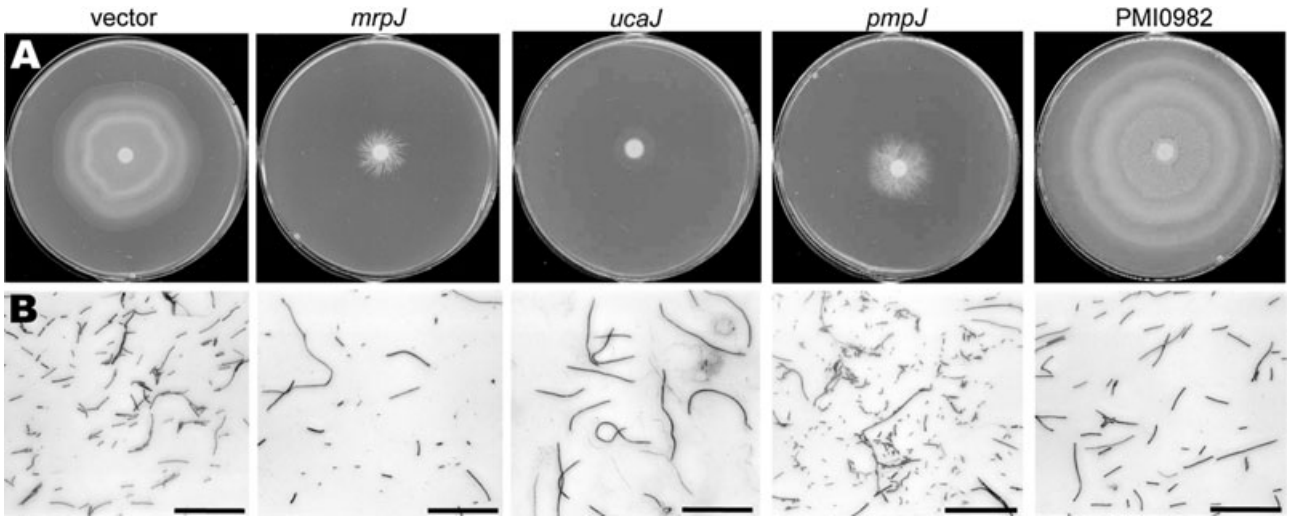


**Fig. 3.** A. Representative swarming phenotypes of strain HI4320 expressing *mrpJ* paralogues.
B. Gram stains of bacteria taken from the edge of swarm fronts. The reference bar is 50 μm.

(Fig. 2), most bacteria in the population lacked a flagellum (Fig. 4D). In contrast, many of the vector control or PMI0982 overexpression bacteria expressed intact flagella (Fig. 4A and E).

All the five strains examined by TEM expressed abundant fimbriae (Fig. 4). Many of these fimbriae were seen as sheared fragments in the background. Intriguingly, the appearance of individual fimbriae varied between the different overexpression strains. Specifically, the *mrpJ* overexpression strain possessed relatively short, thick fimbriae (Fig. 4B) while the fimbriae on the *ucaJ* overexpression strain (Fig. 4C) were predominantly long, thin and straight compared with the vector control.

### *The predicted HTH region of MrpJ is required for MrpJ function*

To locate the amino acid residues of MrpJ critical for its function, MrpJ and the predicted sequences of the other 14 paralogues were aligned using the CLUSTALW algorithm (Fig. 5A). Three residues are conserved in all 15 proteins; in MrpJ, these are R27, Q46 and E52. An additional 20 amino acids are conserved in at least 9 of 15 MrpJ-type proteins encoded by HI4320 (Fig. 5A, orange and green residues in the consensus sequence). A core region of conserved amino acids in MrpJ, SQQQFSRYE (Fig. 5B, green residues), was identified as a likely critical motif within this protein. Each of these MrpJ amino acids was substituted with Ala using site-directed mutagenesis of the *mrpJ* overexpression plasmid pLX3805. All site-directed mutants had significantly increased swimming motility compared with the *mrpJ* control ($P < 0.05$) except for the Q47A mutant (Fig. 6A), confirming the importance of these amino acids for the function of MrpJ. The nine additional conserved amino acid residues located outside the core conserved region (Fig. 5B, blue residues) were changed to Asp residues and examined for swimming motility (Fig. 6A). All nine mutants had significantly increased swimming motility compared with the vector control ($P < 0.05$).

To further localize regions of MrpJ necessary for function, 15 nt linkers were inserted randomly into *mrpJ*. Twenty-eight unique in-frame insertion mutants (Fig. 5B, black arrows; see also Fig. S1) were measured for swimming motility (Fig. 6B). Mutations within a region corresponding to the predicted HTH domain of MrpJ (Fig. 5B) had the greatest effect on swimming motility (Fig. 6B, mutant 221 to mutant 1). Seven *mrpJ* mutants with insertions that result in premature stop codons (Fig. 5B, red arrows) were also examined for swimming motility (Fig. 6C).

Deletion of the C-terminal 27 amino acids of 110-amino-acid MrpJ (Fig. 6C and Fig. S1, mutant 211) had no effect on MrpJ function. Deletion of the C-terminal 37 amino acids of MrpJ (Fig. 6C and Fig. S1, mutant 133) resulted in a partial loss of MrpJ function (Fig. 6C, compare uninduced and induced expression of mutant 133); only when the C-terminal 45 amino acids (41% of MrpJ) were removed (Fig. 6C and Fig. S1, mutant 32) was the MrpJ protein unable to function.

### *MrpJ binds the promoter region of* flhDC

$FlhD_2C_2$ is the master regulator of the flagellar operon (Macnab, 1996). To determine whether MrpJ controls motility by regulating $FlhD_2C_2$, the promoter region of *flhDC* was amplified by PCR, labelled and used as a target in electrophoretic mobility shift assays (Fig. 7A).

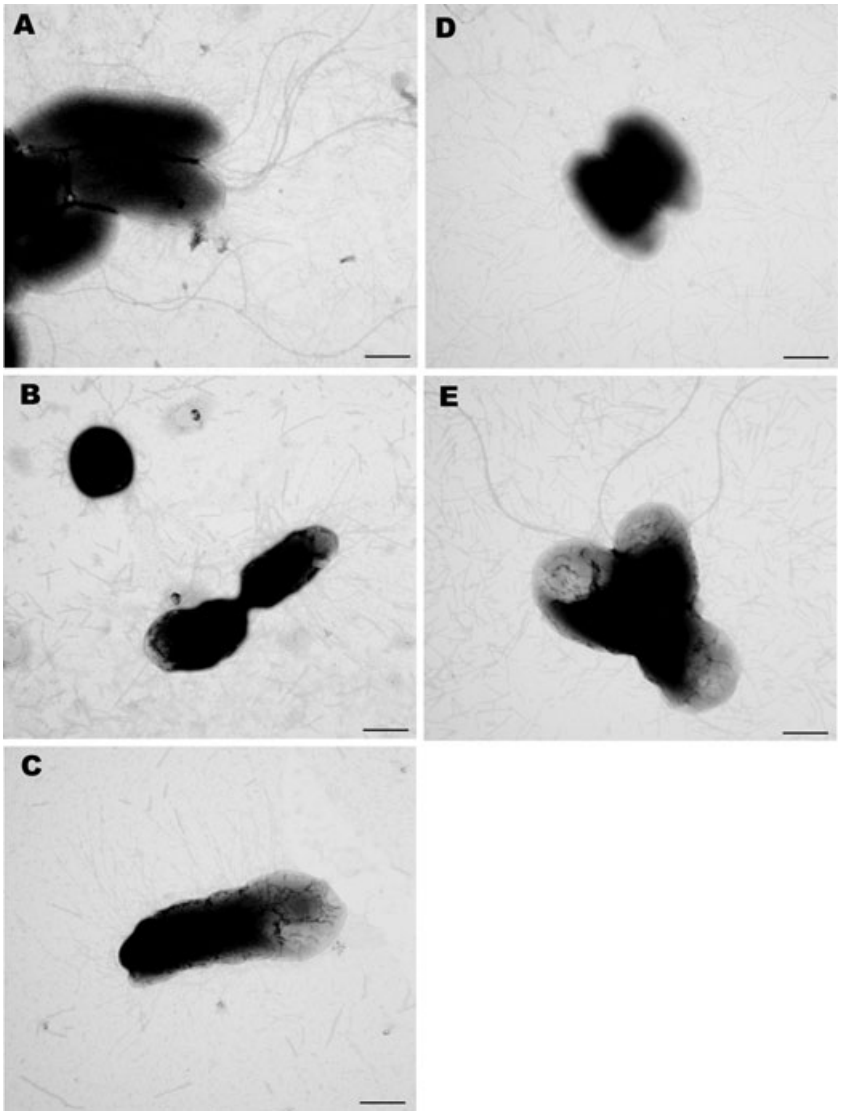


**Fig. 4.** TEM of *P. mirabilis* strains overexpressing *mrpJ* paralogues. Flagella are the long, whip-like structures seen in A and E, while fimbriae are the shorter, thinner structures visible in all five panels. (A) Empty vector control; (B) *mrpJ*; (C) *ucaJ*; (D) *pmpJ*; (E) PMI0982.

Addition of MrpJ-$His_6$ to the *flhDC* promoter (Fig. 7A, lanes 3–7) resulted in a retardation of the mobility of the DNA compared with the promoter alone. In contrast, there was no mobility shift when MrpJ-$His_6$ was added to the *flhD* coding sequence (Fig. 7A, lanes 1–2).

To confirm that MrpJ regulates *flhDC*, quantitative reverse transcriptase PCR (qRT-PCR) was used to measure *flhD* and *flaA* (flagellin) transcript levels in the presence or absence of the *mrpJ* overexpression plasmid pLX3805 (Fig. 7B). Indeed, overexpression of *mrpJ* led to an average 3.3-fold decrease in *flhD* transcript and an average 19.1-fold decrease in *flaA* transcript (Fig. 7B).

To test whether other MrpJ paralogues might bind the *flhDC* promoter, UcaJ-$His_6$ was purified and added to the *flhDC* promoter (Fig. 7C). As expected, addition of increasing amounts of UcaJ-$His_6$ to the *flhDC* promoter led to a corresponding decrease in DNA mobility compared with the promoter alone.

## Discussion

The fact that *P. mirabilis* HI4320 possesses 15 copies of *mrpJ* demonstrates that this bacterium is committed to tightly regulating expression of flagella for motility versus fimbriae for adherence. MrpJ and its homologues are transcriptional regulators of the bacterial XRE family, defined by the presence of a DNA-binding HTH domain. Alignment of the predicted protein sequences of all 15 *mrpJ*-type genes in *P. mirabilis* revealed that the conserved amino acid consensus sequence motif within these proteins is consistently located within the HTH domain. Mutation of individual conserved amino acid residues, coupled with data from linker insertion mutagenesis of *mrpJ*, confirmed the critical contribution of the HTH domain in MrpJ function. This family of regulators likely mediates repression of motility by direct binding to the flagellar master regulator $FlhD_2C_2$, resulting in repression

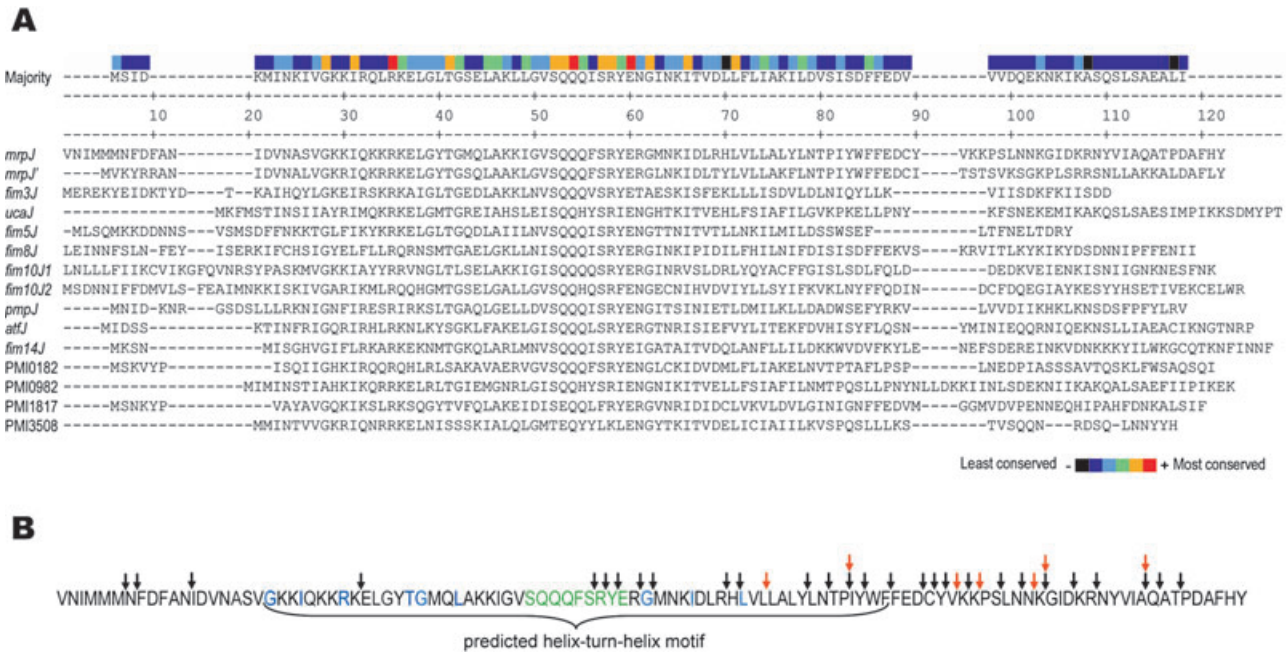


**Fig. 5.** Identification and mutation of conserved amino acid residues of MrpJ.
A. Alignment of MrpJ and the 14 *P. mirabilis* MrpJ paralogues. The CLUSTALW algorithm was used to align the amino acid sequences of MrpJ with its paralogues. The consensus sequence is shown in the first line. The degree of amino acid conservation is shown at the top, with highly conserved amino acids indicated in red or orange.
B. Location of mutations in MrpJ. Site-directed mutations in amino acids conserved among MrpJ and its paralogues are highlighted in green (Ala substitution) and blue (Asp substitution). The locations of 5 aa in-frame insertions are indicated by black arrows, while 5 aa insertions that result in premature stop codons are indicated by red arrows. The predicted HTH domain of MrpJ is indicated with a bracket.

of its transcription and the downregulation of flagellar synthesis. When any of the 10 fimbrial operons that carry an active MrpJ paralogue are expressed, motility will be dramatically downregulated. Thus the opposing forces of motility and adherence are minimized by the action of MrpJ paralogues.

The presence of 15 copies of *mrpJ*-type genes in *P. mirabilis*, in retrospect, likely explains why the original *mrpJ* deletion strain had no apparent phenotype (Li *et al.*, 2001). However, it is possible that not all the *mrpJ* paralogues function in the same way, or that they regulate overlapping but not identical pathways. This possibility is suggested by the unique swarming patterns (Fig. 3) and different fimbrial appearances (Fig. 4) of *mrpJ* paralogue overexpression strains. Additionally, the two *mrpJ* paralogues that had very little effect on motility, PMI0182 and PMI0982, may either be non-functional or regulate other pathways beside motility. Examination of the predicted protein sequences of PMI0182 and PMI0982 reveals an arginine residue that is conserved in these two proteins, yet is not found in the other 13 MrpJ proteins (Fig. 5A, residue 39 of the consensus sequence). Although all *mrpJ* paralogue clones grow at the same rate as the vector control when uninduced, it should be noted that many strains, including the *mrpJ* overexpression strain, have a significant growth lag when induced with 0.3 mM IPTG (data not shown). Yet, Western blot analysis demonstrates that levels of the major flagellin FlaA are clearly reduced in most *mrpJ* overexpression strains, even when overexpression was not induced. Therefore, reduced swimming motility radii in induced strains are likely a combined result of reduced flagellar expression and slower growth.

The full mechanism of MrpJ regulation remains unknown. Because MrpJ decreases the amount of flagella produced by *P. mirabilis*, we predicted that MrpJ binds the promoter of the flagellar master regulator, *flhDC*. However, Li *et al.* (2001) reported that His-tagged MrpJ does not bind these sequences. There are several possible explanations for our current finding that MrpJ actually does bind the *flhDC* promoter. Primarily, in this study, a larger fragment of the region upstream of *flhDC* was assessed for MrpJ binding (550 nt compared with 400 nt). It is also possible that the shift was not detected because of poorer resolution or less sensitive detection; in the current study, chemiluminescent detection was used on fragments separated on a polyacrylamide gel, while the previous report used ethidium bromide detection on fragments separated with an agarose gel. There is a large distance (2757 nt) between *flhD* and the next gene (PMI1673, a hypothetical gene), providing possible sites for multiple regulators to bind this region. Although MrpJ

 

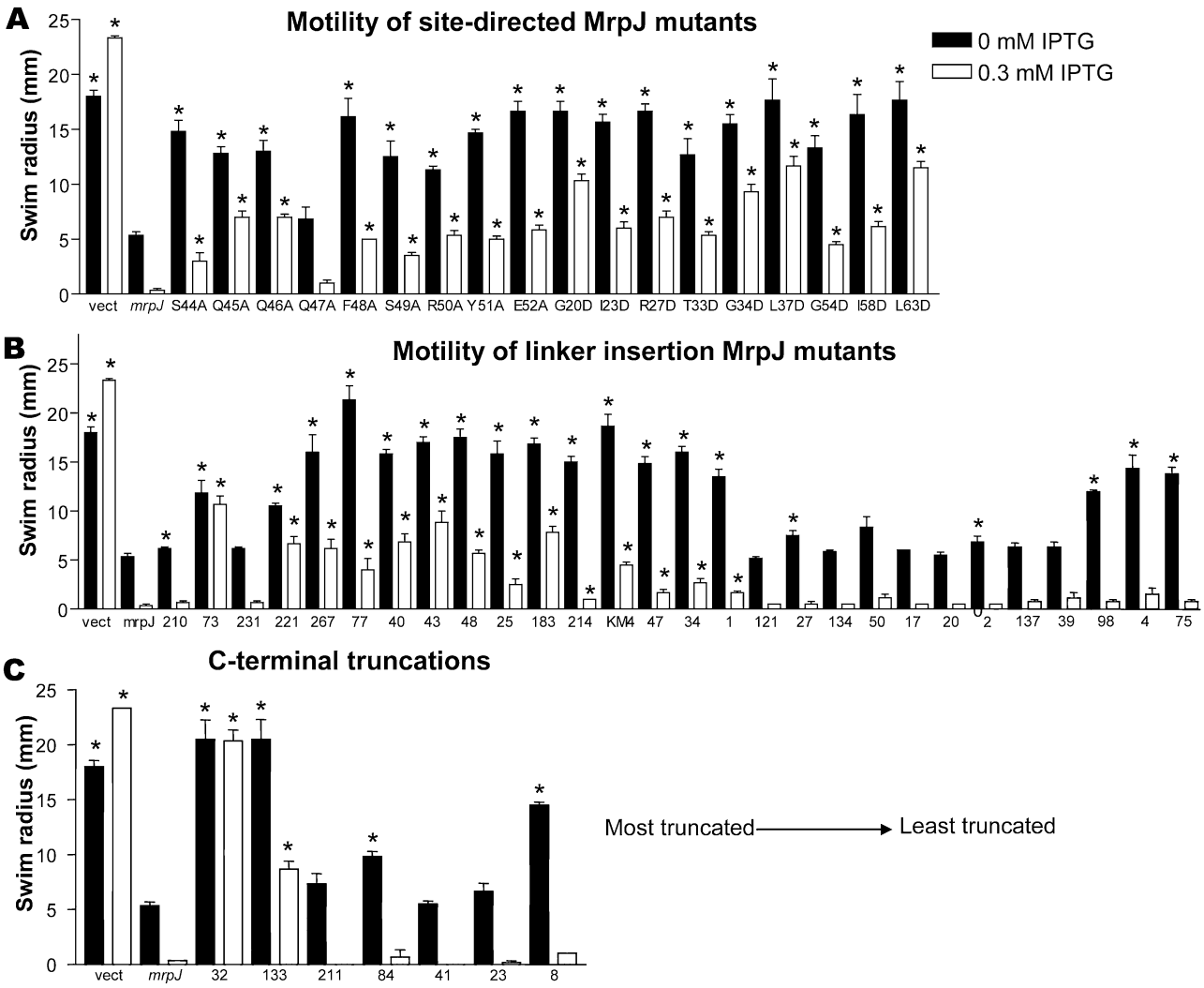


**Fig. 6.** Swimming motility of HI4320ΔmrpJ overexpressing mutated forms of *mrpJ*. MrpJ mutants were stabbed into soft agar and the radius of motility was measured.
A. Amino acids conserved in MrpJ and its paralogues were substituted with Ala or Asp.
B. Transposon mutagenesis was used to introduce random 5 aa insertions in MrpJ. Mutations are listed in order from N-terminal to C-terminal.
C. Random insertions that resulted in premature stop codons in *mrpJ*. Mutants are listed from most to least truncated. In all panels, black bars represent swarm or swim radii of uninduced strains, while white bars represent strains that were induced with IPTG. Asterisks (*) indicate $P < 0.05$ when compared with the *mrpJ* control. Error bars represent the standard error of the mean.

and most of its paralogues act to reduce expression of *flhDC*, the different contributions of each paralogue to swarming motility suggest that MrpJ likely also acts on other pathways. It is worth noting that the role of the C terminus of MrpJ remains undetermined, particularly as it was possible to delete the C-terminal quarter of MrpJ and still repress motility. A future area of focus will be using unbiased methods to locate other genes that are regulated by MrpJ.

Little is currently known about regulation of the 17 different potential fimbriae encoded by *P. mirabilis*. MR/P fimbriae are preferentially expressed *in vitro* during static culture at 37°C and are expressed during urinary tract infection in mice (Bahrani *et al.*, 1991). Expression of MR/P fimbriae is controlled by an invertible element in the *mrp* promoter (Zhao *et al.*, 1997) which is in turn regulated by the MrpI recombinase (Li *et al.*, 2002). UCA/NAF have been isolated from *P. mirabilis* cultured in minimal medium (Wray *et al.*, 1986) as well as *P. mirabilis* grown on Luria–Bertani (LB) agar plates grown at 37°C (Tolson *et al.*, 1995), but expression was not detected at 23°C (Tolson *et al.*, 1995). Both MR/P fimbriae and UCA/NAF were also found to vary in expression within a swarming colony of *P. mirabilis* (Latta *et al.*, 1999). The ATF are preferentially expressed during static culture at 23°C in rich medium, but not culture at 42°C in minimal medium, or when grown on

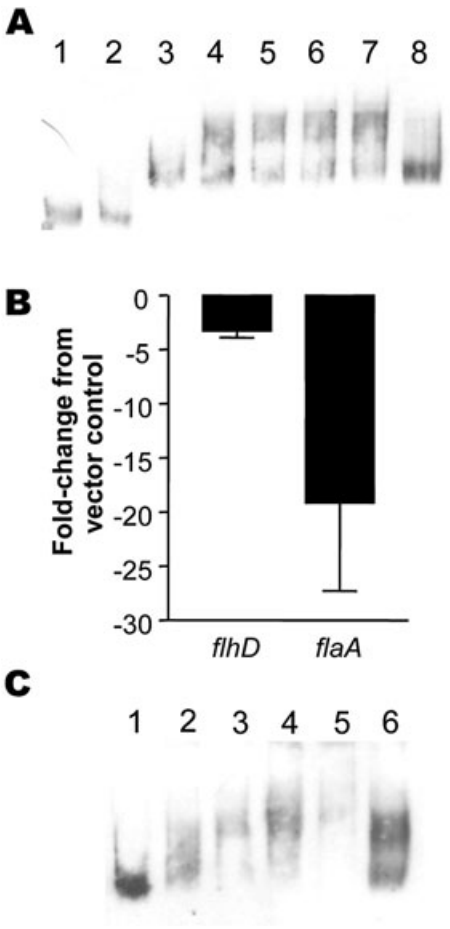


**Fig. 7.** MrpJ directly regulates *flhDC* expression.
A. Gel shift of the *flhDC* promoter by MrpJ-His$_6$. MrpJ-His$_6$ was added to either the DIG-labelled *P. mirabilis flhD* coding sequence or the putative *flhDC* promoter sequence; DNA–protein interactions were detected by retardation of electrophoretic mobility of DNA relative to unbound DNA in a native polyacrylamide gel. Lanes: 1, *flhD* coding sequence DNA (0.4 ng) only; 2, *flhD* DNA plus 320 ng of MrpJ-His$_6$; 3, *flhD* promoter sequence DNA (0.4 ng) only; 4, DNA plus 40 ng of MrpJ-His$_6$; 5, DNA plus 80 ng of MrpJ-His$_6$; 6, DNA plus 160 ng of MrpJ-His$_6$; 7, DNA plus 320 ng of MrpJ-His$_6$; 8, DNA plus 160 ng of MrpJ-His$_6$ plus 200-fold excess unlabelled DNA.
B. Effect of *mrpJ* overexpression on flagellar master regulator *flhD* and flagellin *flaA* transcripts. qRT-PCR was used to compare transcript levels of *flhD* and *flaA* in HI4320 overexpressing *mrpJ* with the HI4320 vector control. The *y*-axis shows the fold change of *flhD* or *flaA* transcripts in the *mrpJ* overexpression strain compared with the vector control. The data are from three independent experiments. Error bars represent the standard error of the mean.
C. Gel shift of the *flhDC* promoter by UcaJ-His$_6$. UcaJ-His$_6$ was added to the DIG-labelled *P. mirabilis* putative *flhDC* promoter sequence. Lanes: 1, *flhD* promoter sequence DNA (0.4 ng) only; 2, DNA plus 150 ng of UcaJ-His$_6$; 3, DNA plus 300 ng of UcaJ-His$_6$; 4, DNA plus 600 ng of UcaJ-His$_6$; 5, DNA plus 1200 ng of UcaJ-His$_6$; 6, DNA plus 600 ng of UcaJ-His$_6$ plus 200-fold excess unlabelled DNA.

solid medium (Massad *et al.*, 1994b). Mannose-resistant/*Klebsiella*-like (MR/K) fimbriae, which are likely PMF (Bahrani *et al.*, 1993), are known to be produced during static culture (Adegbola *et al.*, 1983); however, because MR/K fimbriae were only characterized by erythrocyte binding (i.e. haem-agglutination) and not by protein or nucleotide sequence analysis, it is not certain that the fimbriae analysed were truly PMF. PMP expression has been confirmed by N-terminal sequencing of purified *P. mirabilis* fimbrial protein (Bijlsma *et al.*, 1995), although the culture condition used was not specified. The remaining 12 potential fimbriae encoded by *P. mirabilis* (Pearson *et al.*, 2008) remain uncharacterized. Multiple types of fimbriae can be expressed simultaneously (Adegbola *et al.*, 1983; Bahrani and Mobley, 1993; Massad *et al.*, 1994b; Tolson *et al.*, 1995). It is intriguing to consider whether MrpJ or its paralogues may contribute to regulation of fimbrial expression in addition to regulation of flagella, particularly in light of the different fimbrial appearances exhibited by *mrpJ* or *ucaJ* overexpression strains (Fig. 4).

Although *mrpJ* homologues are found, in a few instances, associated with fimbrial operons in other species (Li *et al.*, 2001; He *et al.*, 2004; Meslet-Cladiere *et al.*, 2004), this unusual method of motility regulation has been embraced by *P. mirabilis* to modulate expression of its surface appendages. This organism is notorious for its ability to swarm over surfaces, morphing alternately between swarmer cells with abundant flagella and fimbriated swimmer cells expressing only a few flagella. Notably, swarm cells have reduced expression of fimbriae (Mobley *et al.*, 1996). Additionally, this organism possesses the machinery to make up to 17 distinct chaperone-usher fimbriae (Pearson *et al.*, 2008). Indeed, 10 fimbrial operons include an *mrpJ* paralogue, emphasizing the idea that when *P. mirabilis* is adherent, it seeks to downregulate motility. The exact mechanisms for *mrpJ* control of motility and swarm cell downregulation of fimbriae will make interesting future directions of study.

## Experimental procedures

### *Bacterial strains and culture conditions*

*P. mirabilis* HI4320 was isolated from the urine of an elderly, long-term catheterized woman (Mobley and Warren, 1987). *E. coli* DH5α was used as the host strain for cloning of *mrpJ* paralogues and *mrpJ* mutagenesis experiments. All strains and mutants were cultured at 37°C in non-swarming LB broth ($l^{-1}$: 10 g tryptone, 5 g yeast extract, 0.5 g NaCl) or on LB medium solidified with 1.5% agar. Antibiotic supplementation of chloramphenicol (20 μg ml$^{-1}$), ampicillin (100 μg ml$^{-1}$) or kanamycin (25 μg ml$^{-1}$) was provided as necessary.

### *Cloning of* mrpJ *paralogues*

The IPTG-inducible plasmid pLX3607 and *mrpJ* overexpression plasmid pLX3805 have been described (Li *et al.*, 2001). The 14 additional *mrpJ* paralogues in the HI4320 genome were amplified by PCR (primers in Table S1) and cloned into the NcoI and HindIII sites of pLX3607 (Table 2), with the

**Table 2.** Plasmids used in this study.

| Name | Description | Source |
|---|---|---|
| pLX3607 | IPTG-inducible cloning vector; amp$^R$ | Li et al. (2001) |
| pLX3805 | pLX3607 with *mrpJ* in the NcoI-HindIII sites | Li *et al.* (2001) |
| pMP123 | pLX3607 with *mrpJ'* in the NcoI-HindIII sites | This study |
| pMP124 | pLX3607 with *fim3J* in the NcoI-HindIII sites | This study |
| pMP125 | pLX3607 with *ucaJ* in the NcoI-HindIII sites | This study |
| pMP126 | pLX3607 with *fim5J* in the NcoI-HindIII sites | This study |
| pMP128 | pLX3607 with *pmpJ* in the NcoI-HindIII sites | This study |
| pMP129 | pLX3607 with *atfJ* in the NcoI-HindIII sites | This study |
| pMP131 | pLX3607 with *fim10J2* in the NcoI-HindIII sites | This study |
| pMP165 | pLX3607 with *fim14J* in the NcoI-HindIII sites | This study |
| pMP183 | pLX3607 with *fim8J* in the NcoI-HindIII sites | This study |
| pMP184 | pLX3607 with *fim10J1* in the NcoI-HindIII sites | This study |
| pMP185 | pLX3607 with PMI0182 in the NcoI-HindIII sites | This study |
| pMP186 | pLX3607 with PMI0982 in the NcoI-HindIII sites | This study |
| pMP187 | pLX3607 with PMI1817 in the NcoI-HindIII sites | This study |
| pMP188 | pLX3607 with PMI3508 in the NcoI-HindIII sites | This study |
| pLX2501 | pLX3607 with *mrpJ* in the NcoI-BglII sites; His-tag | Li *et al.* (2001) |
| pMP201 | pBAD/*Myc*-HisA with *ucaJ* in the NcoI-HindIII sites; His-tag | This study |

exception of *fim3J*, which was cloned into the NcoI and BamHI sites of pLX3607. After all sequences were confirmed by nucleotide sequence analysis, wild-type *P. mirabilis* HI4320 was electroporated with each of the plasmids.

### *Swimming and swarming motility assays*

Swimming motility was assessed by stabbing a swim plate (1% tryptone, 0.5% NaCl, 0.25% agar) with a late logarithmic phase bacterial culture ($OD_{600}$ = 1.0). Care was taken not to stab through to the bottom of the plate, to prevent twitching motility. Swim plates were incubated for 19 h at 30°C before the radius of motility was measured. Swarming motility was assessed by spotting 5 μl of late logarithmic phase bacterial culture ($OD_{600}$ = 1.0) onto the centre of a swarm plate (1% tryptone, 1% NaCl, 0.5% yeast extract, 1.5% agar). Swarm plates were incubated inverted at 30°C for 17 h before the radius of motility was measured. Ampicillin (100 μg ml$^{-1}$) was added to plates as necessary to maintain overexpression plasmids. All results represent the mean of three independent experiments. The paired *t*-test was used to compare motility radii with either the vector or *mrpJ* controls; one-tailed *P*-values < 0.05 were considered significant.

### *Western blot analysis*

Overnight, aerated cultures of HI4320 with overexpression plasmids containing *mrpJ* or its paralogues were adjusted to $OD_{600}$ = 1.0. Alternatively, cultures were grown to mid-logarithmic phase ($OD_{600}$ = 0.6). Cultures were not induced with IPTG. A 1 ml sample of each culture was collected by centrifugation (6000 *g*, 8 min). The bacterial cell pellet was suspended in 100 μl of 2× Laemmli sample buffer, boiled for 10 min and separated by SDS-PAGE. Western blot analysis was conducted using anti-FlaA antibody (Mobley *et al.*, 1996) or anti-UreD antibody (Heimer and Mobley, 2001) as previously described and peroxidase-conjugated goat anti-rabbit IgG (Sigma) as the secondary antibody. Chemiluminescence was accomplished using the ECL Plus Western Blotting Detection System (Amersham, GE Healthcare) according to the manufacturer's directions.

### *DNA sequencing and analysis*

DNA sequencing was performed by the University of Michigan DNA sequencing core. Sequences were analysed using the DNASTAR Lasergene suite software, version 7.0. Translated *mrpJ* paralogues were aligned using the CLUSTALW algorithm in Lasergene.

### *Transmission electron microscopy*

Ten microlitres of an overnight culture was added to the surface of 300 mesh copper grids (Electron Microscopy Sciences) and allowed to bind for 3 min. Liquid was wicked off with filter paper, and 10 μl of fixative (2.5% glutaraldehyde, 2% paraformaldehyde in PBS) was added to each grid for 5 min. Grids were dipped in distilled water 10 times, and a 1% phosphotungstic acid stain was applied for 30 s. Remaining liquid was wicked away with filter paper, and the grids were allowed to dry for 10 min. Grids were viewed using a Philips CM-100 transmission electron microscope.

### *Mutagenesis of* mrpJ

Site-directed mutagenesis of *mrpJ* was accomplished using the QuikChange II site-directed mutagenesis kit (Stratagene) according to the manufacturer's directions (mutagenic primers in Table S2). Random 15 nt insertions in *mrpJ* were constructed using the GPS-LS linker scanning system (NEB) according to the manufacturer's protocol. In both cases, the *mrpJ* overexpression plasmid pLX3805 was used as the template for mutagenesis. Mutation of pLX3805 was confirmed using nucleotide sequence analysis. Mutated *mrpJ* plasmids were introduced to the *mrpJ*-null mutant HI4320Δ*mrpJ* by electroporation.

 

### *Electrophoretic mobility shift assays*

Purification of His-tagged MrpJ protein from *E. coli* M15 containing pLX2501 has been described (Li *et al*., 2001). His-tagged UcaJ protein was obtained by cloning *ucaJ* into the NcoI and HindIII sites of pBAD/*Myc*-His A (Invitrogen) and purifying using the same method of Li *et al.* (2001). Purified protein was desalted using 3500 MWCO dialysis cassettes (Pierce). Gel shifts using the PCR-amplified gene promoter region of *flhDC* or the *flhD* coding sequence (primers in Table S3), and MrpJ-$His_6$ or UcaJ-$His_6$ were accomplished using the DIG gel shift kit (Roche) according to the manufacturer's recommendations.

### *Quantitative reverse transcriptase PCR*

HI4320 containing pLX3607 or pLX3805 (+*mrpJ*) was cultured overnight in LB broth supplemented with ampicillin. These cultures were diluted 1:100 into fresh medium and grown to logarithmic phase ($OD_{600}$ = 1.0). RNA protect (2 ml) (Qiagen) was added to 1 ml of culture, and RNA was isolated using the RNeasy kit (Qiagen) according to the manufacturer's instructions. DNA was digested using Turbo-DNA*free* DNase (Ambion). RNA was used as the template for cDNA synthesis using the Superscript First-Strand Synthesis System (Invitrogen) according to the manufacturer's protocol. PCR with primers specific to the *rpoA* gene (RNA polymerase A) was performed on cDNA samples prepared with and without reverse transcriptase to ensure no genomic DNA contamination of the RNA preparations. Each qRT-PCR reaction was set up in duplicate and consisted of 30 ng cDNA template, 150 nM of each primer and 12.5 µl 2× SYBR Green PCR master mix (Stratagene). Target genes were amplified using an Mx3000P thermal cycler (Stratagene). Melting curve analysis was used to confirm a lack of primer dimers or genomic DNA contamination of reagents. Data were normalized to *rpoA*, and analysed by the $2^{-\Delta\Delta}CT$ method (Livak and Schmittgen, 2001). Primers used for qRT-PCR are listed in Table S3.

## Acknowledgements

The authors thank Dotty Sorenson of the Microscopy and Image Analysis Laboratory at the University of Michigan for expert assistance with TEM. This work was funded by Public Health Service Grant AI059722 from the National Institutes of Health (H.L.T.M.). M.M.P. was supported in part by the Molecular Mechanisms of Microbial Pathogenesis Training Grant (T32 AI7528) and National Research Service Award F32 AI068324.

## References

Adegbola, R.A., Old, D.C., and Senior, B.W. (1983) The adhesins and fimbriae of *Proteus mirabilis* strains associated with high and low affinity for the urinary tract. *J Med Microbiol* **16:** 427–431.

Akerley, B.J., Cotter, P.A., and Miller, J.F. (1995) Ectopic expression of the flagellar regulon alters development of the *Bordetella*–host interaction. *Cell* **80:** 611–620.

Bahrani, F.K., and Mobley, H.L. (1993) *Proteus mirabilis* MR/P fimbriae: molecular cloning, expression, and nucleotide sequence of the major fimbrial subunit gene. *J Bacteriol* **175:** 457–464.

Bahrani, F.K., Johnson, D.E., Robbins, D., and Mobley, H.L. (1991) *Proteus mirabilis* flagella and MR/P fimbriae: isolation, purification, N-terminal analysis, and serum antibody response following experimental urinary tract infection. *Infect Immun* **59:** 3574–3580.

Bahrani, F.K., Cook, S., Hull, R.A., Massad, G., and Mobley, H.L. (1993) *Proteus mirabilis* fimbriae: N-terminal amino acid sequence of a major fimbrial subunit and nucleotide sequences of the genes from two strains. *Infect Immun* **61:** 884–891.

Bahrani, F.K., Massad, G., Lockatell, C.V., Johnson, D.E., Russell, R.G., Warren, J.W., and Mobley, H.L. (1994) Construction of an MR/P fimbrial mutant of *Proteus mirabilis*: role in virulence in a mouse model of ascending urinary tract infection. *Infect Immun* **62:** 3363–3371.

Bijlsma, I.G., van Dijk, L., Kusters, J.G., and Gaastra, W. (1995) Nucleotide sequences of two fimbrial major subunit genes, *pmpA* and *ucaA*, from canine-uropathogenic *Proteus mirabilis* strains. *Microbiology* **141** (Part 6)**:** 1349–1357.

Bryan, A., Roesch, P., Davis, L., Moritz, R., Pellett, S., and Welch, R.A. (2006) Regulation of type 1 fimbriae by unlinked FimB- and FimE-like recombinases in uropathogenic *Escherichia coli* strain CFT073. *Infect Immun* **74:** 1072–1083.

Clegg, S., and Hughes, K.T. (2002) FimZ is a molecular link between sticking and swimming in *Salmonella enterica* serovar Typhimurium. *J Bacteriol* **184:** 1209–1213.

Coker, C., Poore, C.A., Li, X., and Mobley, H.L. (2000) Pathogenesis of *Proteus mirabilis* urinary tract infection. *Microbes Infect* **2:** 1497–1505.

Cook, S.W., Mody, N., Valle, J., and Hull, R. (1995) Molecular cloning of *Proteus mirabilis* uroepithelial cell adherence (*uca*) genes. *Infect Immun* **63:** 2082–2086.

Finlay, B.B., and Falkow, S. (1997) Common themes in microbial pathogenicity revisited. *Microbiol Mol Biol Rev* **61:** 136–169.

Gardel, C.L., and Mekalanos, J.J. (1996) Alterations in *Vibrio cholerae* motility phenotypes correlate with changes in virulence factor expression. *Infect Immun* **64:** 2246–2255.

He, H., Snyder, H.A., and Forst, S. (2004) Unique organization and regulation of the *mrx* fimbrial operon in *Xenorhabdus nematophila*. *Microbiology* **150:** 1439–1446.

Heimer, S.R., and Mobley, H.L. (2001) Interaction of *Proteus mirabilis* urease apoenzyme and accessory proteins identified with yeast two-hybrid technology. *J Bacteriol* **183:** 1423–1433.

Jansen, A.M., Lockatell, C.V., Johnson, D.E., and Mobley, H.L. (2003) Visualization of *Proteus mirabilis* morphotypes in the urinary tract: the elongated swarmer cell is rarely observed in ascending urinary tract infection. *Infect Immun* **71:** 3607–3613.

Lane, M.C., Simms, A.N., and Mobley, H.L. (2007) Complex interplay between type 1 fimbrial expression and flagellum-mediated motility of uropathogenic *Escherichia coli*. *J Bacteriol* **189:** 5523–5533.

Latta, R.K., Grondin, A., Jarrell, H.C., Nicholls, G.R., and Bérubé, L.R. (1999) Differential expression of nonaggluti-

 

nating fimbriae and MR/P pili in swarming colonies of *Proteus mirabilis*. *J Bacteriol* **181:** 3220–3225.
Li, X., Rasko, D.A., Lockatell, C.V., Johnson, D.E., and Mobley, H.L. (2001) Repression of bacterial motility by a novel fimbrial gene product. *EMBO J* **20:** 4854–4862.
Li, X., Lockatell, C.V., Johnson, D.E., and Mobley, H.L. (2002) Identification of MrpI as the sole recombinase that regulates the phase variation of MR/P fimbria, a bladder colonization factor of uropathogenic *Proteus mirabilis*. *Mol Microbiol* **45:** 865–874.
Livak, K.J., and Schmittgen, T.D. (2001) Analysis of relative gene expression data using real-time quantitative PCR and the 2(-Delta Delta C(T)) Method. *Methods* **25:** 402.
Macnab, R.M. (1996) Flagella and motility. In *Escherichia coli and Salmonella: Cellular and Molecular Biology*. Neidhardt, F.C. (ed.). Washington, DC: American Society for Microbiology Press, pp. 123–145.
Massad, G., Lockatell, C.V., Johnson, D.E., and Mobley, H.L. (1994a) *Proteus mirabilis* fimbriae: construction of an isogenic *pmfA* mutant and analysis of virulence in a CBA mouse model of ascending urinary tract infection. *Infect Immun* **62:** 536–542.
Massad, G., Bahrani, F.K., and Mobley, H.L. (1994b) *Proteus mirabilis* fimbriae: identification, isolation, and characterization of a new ambient-temperature fimbria. *Infect Immun* **62:** 1989–1994.
Meslet-Cladiere, L.M., Pimenta, A., Duchaud, E., Holland, I.B., and Blight, M.A. (2004) *In vivo* expression of the mannose-resistant fimbriae of *Photorhabdus temperata* K122 during insect infection. *J Bacteriol* **186:** 611–622.
Mobley, H.L., and Warren, J.W. (1987) Urease-positive bacteriuria and obstruction of long-term urinary catheters. *J Clin Microbiol* **25:** 2216–2217.
Mobley, H.L., Belas, R., Lockatell, V., Chippendale, G., Trifillis, A.L., Johnson, D.E., and Warren, J.W. (1996) Construction of a flagellum-negative mutant of *Proteus mirabilis*: effect on internalization by human renal epithelial cells and virulence in a mouse model of ascending urinary tract infection. *Infect Immun* **64:** 5332–5340.
Pearson, M.M., Sebaihia, M., Churcher, C., Quail, M.A., Seshasayee, A.S., Luscombe, N.M., *et al.* (2008) The complete genome sequence of uropathogenic *Proteus mirabilis*, a master of both adherence and motility. *J Bacteriol* **190:** 4027–4037.
Rather, P.N. (2005) Swarmer cell differentiation in *Proteus mirabilis*. *Environ Microbiol* **7:** 1065–1073.
Simm, R., Morr, M., Kader, A., Nimtz, M., and Römling, U. (2004) GGDEF and EAL domains inversely regulate cyclic di-GMP levels and transition from sessility to motility. *Mol Microbiol* **53:** 1123–1134.
Tolson, D.L., Barrigar, D.L., McLean, R.J., and Altman, E. (1995) Expression of a nonagglutinating fimbria by *Proteus mirabilis*. *Infect Immun* **63:** 1127–1129.
Wray, S.K., Hull, S.I., Cook, R.G., Barrish, J., and Hull, R.A. (1986) Identification and characterization of a uroepithelial cell adhesin from a uropathogenic isolate of *Proteus mirabilis*. *Infect Immun* **54:** 43–49.
Zhao, H., Li, X., Johnson, D.E., Blomfield, I., and Mobley, H.L. (1997) In vivo phase variation of MR/P fimbrial gene expression in *Proteus mirabilis* infecting the urinary tract. *Mol Microbiol* **23:** 1009–1019.

## Supplementary material

This material is available as part of the online article from:
http://www.blackwell-synergy.com/doi/abs/10.1111/j.1365-2958.2008.06307.x
(This link will take you to the article abstract).

Please note: Blackwell Publishing is not responsible for the content or functionality of any supplementary materials supplied by the authors. Any queries (other than missing material) should be directed to the corresponding author for the article.